



# Quantum dot light-emitting devices

Dmitri V. Talapin and Jonathan Steckel, Guest Editors

Colloidal semiconductor nanocrystals, also known as “quantum dots” (QDs), represent an example of a disruptive technology for display and lighting applications. The QDs’ high luminescence efficiency and precisely tunable, narrow emission are nearly ideal for achieving saturated colors and enriching the display or TV color gamut. Quantum dot light-emitting diodes (QLEDs) can provide saturated emission colors and allow inexpensive solution-based device fabrication on almost any substrate. The first incorporation of QDs into the consumer market is using them as optical down-converters. Blue light from an efficient high energy light source (e.g., GaN blue LED) is absorbed and reemitted at any desired lower energy wavelength. Alternatively, electric current can be used for direct excitation of QDs. QLEDs are an exciting technical challenge and commercial opportunity for display and solid-state lighting applications. Recent developments in the field show that efficiency and brightness of QLEDs can match those of organic LEDs.

## Brief history

Quantum dots (QDs) have attracted interest from scientists and engineers, particularly when it was realized that at nanometer length scales, the color of semiconductor particles depended on their physical size. In the early-1980s, both in the then Soviet Union and the United States, the concept of quantum confinement had emerged theoretically and experimentally.<sup>1,2</sup> Quantum confinement in QDs gives rise to discrete electron and hole states that can be precisely tuned by varying the particle size of the semiconductor QDs (Figure 1a). Efforts to harness this quantum tunability of the QDs have led to many interesting ideas for optical and optoelectronic applications, such as light-emitting devices<sup>3</sup> and luminescent tags for biochemical assays.<sup>4</sup> Before the physics of quantum confinement was even understood, semiconductor QDs were already being used in colored glass for optical filters. These filters often suffered from stray luminescence that caused background noise and artifacts. Ironically, current commercial prospects of colloidal QDs revolve around their amazing luminescence properties.

## What makes quantum dots exceptional emitters?

Confined inside a QD, an electron and a hole can recombine, emitting a photon with energy equal to the gap between the highest occupied and the lowest unoccupied states. Figure 1a shows a photograph of colloidal solutions of CdSe QDs

illuminated with a 365 nm ultraviolet lamp. Despite the wide range of emission wavelengths, all flasks contain nominally the same chemical species. The difference is they are crystallites of different sizes, ranging from about 1.7 nm in the blue-emitting solution to about 5 nm for the red-emitting solution. Proper control of surface chemistry can essentially eliminate the midgap states associated with surface dangling bonds. As a result of the reduced probability of carrier trapping and non-radiative recombination, high (>80%) luminescence quantum efficiencies (the ratios of the number of photons emitted to the number of photons absorbed) have been reported for several QD materials.<sup>5–9</sup> Many chemical developments were necessary to obtain QDs that combined high luminescence efficiency with narrow emission spectra and whose luminescent properties remained stable over a long period of time.

The perception of color purity is directly related to the widths of the emission spectra, which, in turn, is related to the width of the QD size distribution. Obtaining highly monodisperse QD samples, such as one shown in Figure 1b, required an understanding of the nucleation and growth kinetics<sup>10</sup> or mastering size separation procedures.<sup>11</sup> Figure 1c shows typical absorption and emission spectra of CdSe QDs. One striking feature of these materials is their symmetric, nearly Gaussian, emission spectra. The full width at half-maximum (FWHM) of the emission band is as narrow as 20–35 nm. For comparison, inorganic phosphors and organic dyes, the closest competitors of QDs, show emission spectra that are

Dmitri V. Talapin, Department of Chemistry, The University of Chicago, USA; dvtalapin@uchicago.edu  
Jonathan Steckel, QD Vision, Lexington, MA; jsteckel@qdvision.com  
DOI: 10.1557/mrs.2013.204

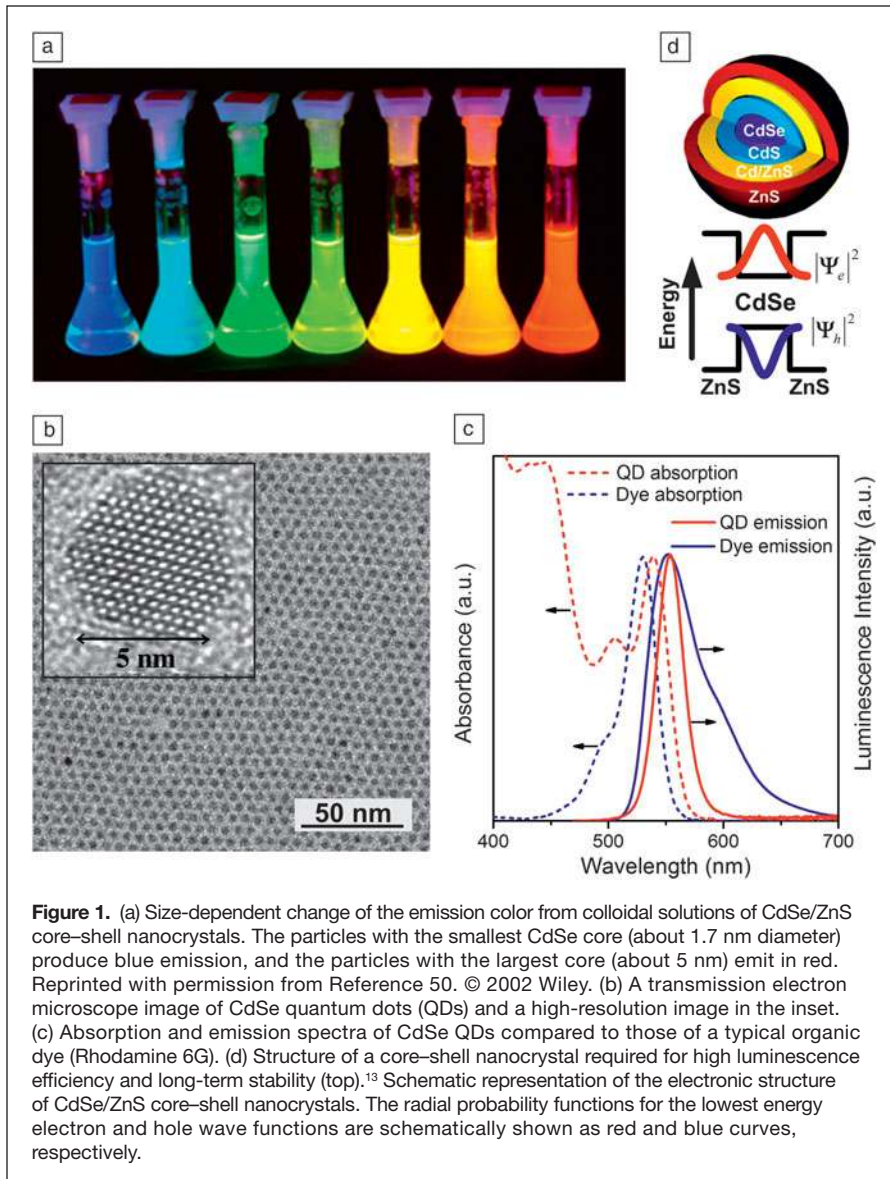


**Figure 1.** (a) Size-dependent change of the emission color from colloidal solutions of CdSe/ZnS core-shell nanocrystals. The particles with the smallest CdSe core (about 1.7 nm diameter) produce blue emission, and the particles with the largest core (about 5 nm) emit in red. Reprinted with permission from Reference 50. © 2002 Wiley. (b) A transmission electron microscope image of CdSe quantum dots (QDs) and a high-resolution image in the inset. (c) Absorption and emission spectra of CdSe QDs compared to those of a typical organic dye (Rhodamine 6G). (d) Structure of a core-shell nanocrystal required for high luminescence efficiency and long-term stability (top).<sup>13</sup> Schematic representation of the electronic structure of CdSe/ZnS core-shell nanocrystals. The radial probability functions for the lowest energy electron and hole wave functions are schematically shown as red and blue curves, respectively.

about twice as broad (Figure 1c). Another fundamental difference between QDs and other luminescent materials lies in the structure of their absorption spectra. The absorption spectra of organic molecules typically contain one or several absorption bands (Figure 1c). In the case of QDs, the absorption cross-section gradually increases at higher energies. Such absorption spectra allow for the simultaneous excitation of QDs with different emission colors using a single blue-emitting light source (Figure 1a).

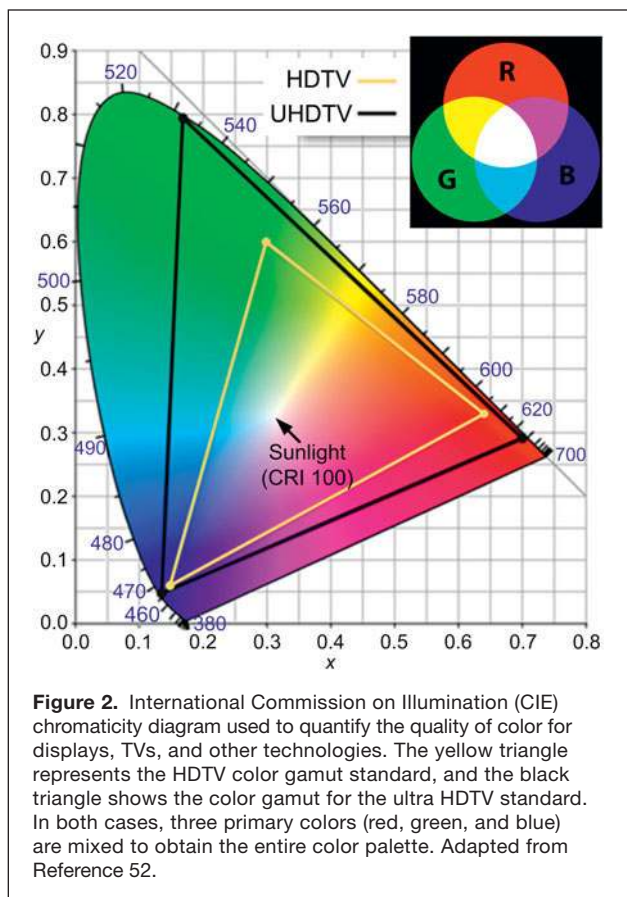
To achieve bright and stable luminescence of QDs, it is necessary to prevent non-radiative recombination pathways usually associated with electron or hole trapping. The dangling bonds at the QD surface are particularly active in the charge-trapping process. These can be eliminated by growing epitaxial heterostructures with core-shell morphology (Figure 1d).<sup>13</sup> The crystalline wide-gap shell helps confine the electron and hole wave functions to the core and eliminates charge trapping at

or near the QD surface. For example, the surfaces of CdSe QDs in Figure 1a are protected by thin (about 1–2 nm) layers of ZnS. In the past decade, the ability to grow thick and uniform shells has been significantly improved.<sup>12</sup> Chemically graded and alloyed shells (e.g., CdSe core and CdS/CdZnS/ZnS layered shell) have reduced strain at the core-shell interface and have further improved structural perfection and luminescence quantum efficiency.<sup>5,13</sup> Originally pioneered by academic labs, these concepts have been further optimized by companies (e.g., QD Corporation, Evident Technologies, QD Vision, Nanosys, Samsung) that work on commercialization of QDs for biomedical, lighting, and now display applications.

### Quantifying color purity, brightness, and luminance

Color purity is arguably the most important competitive advantage of luminescent colloidal QDs. The display industry uses chromaticity diagrams and color gamut standards to quantify this parameter. **Figure 2** shows a frequently used chromaticity diagram established by the International Commission on Illumination (CIE) and referred to as CIE 1931 color space. It maps a range of physically produced colors to an objective description of color sensations by an average human. All the colors accessible to an average human eye are contained inside the diagram. The edge of the diagram is called the spectral locus and represents pure, monochromatic light of a particular wavelength. These are the most saturated colors. The least saturated colors are in

the center of the chromaticity diagram, culminating in white light at the center. The triangles shown in Figure 2 represent two color gamuts, which are the subsets of colors that can be obtained by mixing the colors corresponding to the corners of each triangle. The smaller triangle represents the high definition TV (HDTV) standard, and the larger triangle represents the ultra HDTV (UHDTV) standard approved by the International Telecommunication Union in 2012. All colors within the UHDTV gamut can be obtained by mixing red (630 nm), green (532 nm), and blue (467 nm) primary colors. The narrower the spectral width of the primary colors, the closer the corners of the color triangle will be to the spectral locus. This results in higher color saturation. By using more saturated primary colors, the UHDTV gamut covers 75.8% of the whole color space, while HDTV only has a 35.9% color gamut. The HDTV standard is close to another commonly used gamut standard established by the National Television System Committee (NTSC, 1987).



Practical applications (e.g., LEDs and displays) need to consider the relative sensitivity of the human eye at different wavelengths, which varies significantly across the accessible 400 nm–700 nm spectral range. The brightness is the light power of a source as sensed by the human eye, expressed as the luminous flux ( $F$ ). One lumen ( $lm$ ) is defined as a monochromatic light source emitting an optical power of (1/683) watt at a 555 nm wavelength. For all other wavelengths, the luminous flux can be calculated by multiplying the optical power by the luminosity function  $V(\lambda)$ , which describes the average sensitivity of the human eye to light of different wavelengths.  $V(\lambda)$  is normalized to unity for the peak at  $\lambda = 555$  nm, where the human eye reaches its maximum sensitivity. The luminous intensity unit, candela ( $cd$ ), is defined as one  $lm$  emitting into the solid angle of one steradian. The luminance ( $L_v$ ) is measured in units of  $cd/m^2$  as  $L_v = d^2F/(dA d\Omega \cos\theta)$ , where  $\theta$  is the angle between the surface normal and the specified direction,  $A$  is the area of device surface ( $m^2$ ), and  $\Omega$  is the solid angle ( $sr$ ). **Table I** compares typical luminance of TVs or PC displays, organic LEDs, QLEDs, and inorganic LEDs based on III–V semiconductors.

### Quantum dots as optical down-converters

As shown in Figure 1c, the absorption of QDs increases at short wavelengths irrespective of the emission color. This allows utilizing QDs as optical down-converting materials that

**Table I.** Typical values for luminance of displays, organic LEDs, and inorganic LEDs.<sup>51</sup>

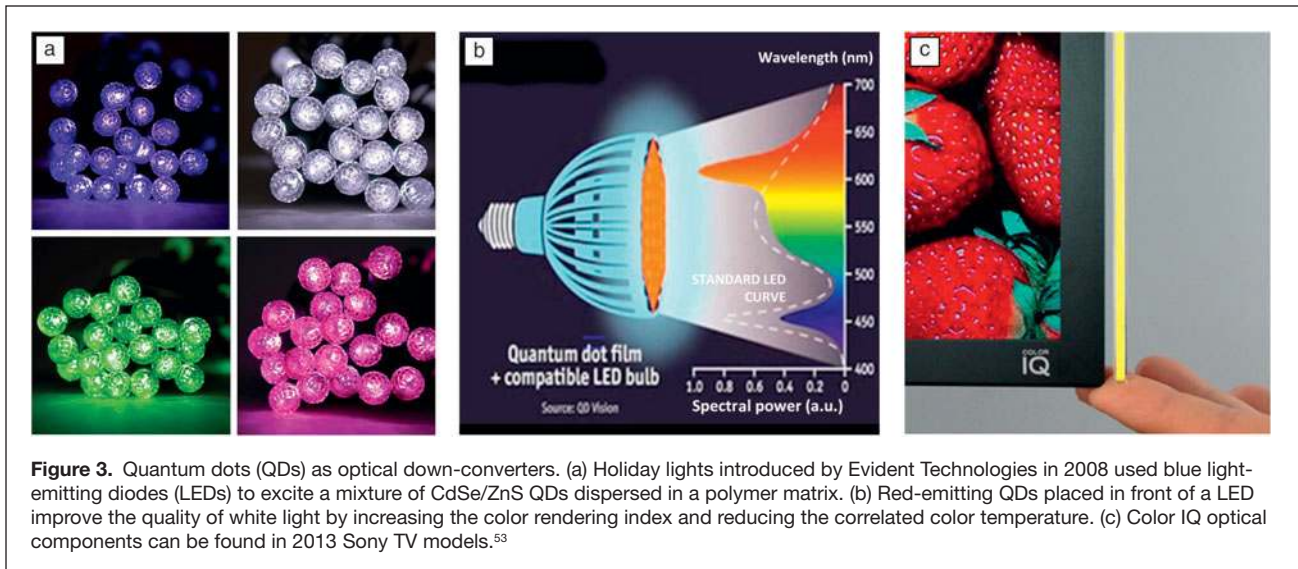
| Device           | Luminance ( $cd/m^2$ ) |
|------------------|------------------------|
| Computer Display | 250–500 (operation)    |
| Computer Display | 1000 (max. value)      |
| III–V LED        | $10^6$ – $10^7$        |
| Organic LEDs     | up to $10^5$           |
| QD LEDs          | $10^5$                 |

efficiently absorb blue light emitted by, for example, a highly efficient InGaN LED. The QDs then convert the blue light into other wavelengths of choice. The process of down-conversion typically involves far-field coupling between re-emitting QDs and the illumination source. However, it can also rely on direct nonradiative Förster-type energy transfer from InGaN quantum wells to the CdSe/ZnS QDs.<sup>14</sup>

Due to the outstanding efficiency of III–V LEDs, the overall performance of a tandem device with QDs can be very good.<sup>15</sup> The efficiency of the down-conversion process is determined by the luminescence quantum efficiency of QDs, which approaches 100% in properly engineered core–shell materials. The key technical challenge is to maintain this high luminescence efficiency of QDs under real operational conditions (i.e., at high excitation fluxes and elevated temperatures). Another important parameter is the efficiency of coupling the emitted light out of the device. This generally depends on the refractive index of the medium in which QDs are dispersed. The light outcoupling efficiency can be enhanced using dielectric mirrors with high reflectivity at the emission band of QDs.<sup>16</sup>

Several important technologies can benefit from using QDs as optical down-converters. The outstanding color purity of QDs allows approaching almost any point on the CIE chromaticity diagram and obtaining colors that are not achievable through the use of traditional phosphors. In 2008, Evident Technologies, Inc. released holiday lights that used blue LEDs to excite CdSe/ZnS QDs dispersed in a polymer cap (**Figure 3a**). These lights were probably the first consumer product utilizing colloidal QD technology.

Due to their spectral purity, QD down-converters can also be used to improve white light generated by LEDs for solid-state lighting. The quality of white light is expressed in terms of correlated color temperature (CCT) and color rendering index (CRI) that compares the LED emission spectrum with the sunlight spectrum corresponding to CRI = 100. Conventional white LEDs generate “cold” white light with CCT > 5000 K and low CRI (about 80–85). To obtain “warmer” looking light that more closely matches the color quality of incandescent lighting, appropriate down-converters should be implemented to enhance the red part of the emission spectrum. Figure 3b shows an example of the addition of red-emitting QDs to a blue LED coated with a yellow phosphor that improves CRI from about 70 to greater than 90 and lowers CCT to a more desirable 2700 K without greatly reducing the device’s luminous efficiency.



In 2009, QD Vision launched the first general lighting product that utilized QDs (Figure 3b). Due to the narrowband red emission of the QDs, these lights were 50% more efficient than the next best high-quality lighting product on the market at the time, at over 60 lm/W.

More recently, QD down-converters are being used for backlighting in LCD displays. This has been made possible by the use of a combination of red and green QDs. Sony, in collaboration with QD Vision, launched the world's first quantum dot television using Color IQ optics in 2013 (Figure 3c). To achieve long-term luminescent stability, QDs were dispersed in an acrylate polymer and encapsulated in thin glass tubes to avoid oxygen exposure. The use of QDs for backlighting increased the color gamut of the LCD displays by 30–40% when compared to traditional white LED backlighting. Optical throughput was also improved, since nearly all of the photons from the excitation source were converted into red, green, and blue primary colors near the color filter transmission peaks. For comparison, in conventional LCD displays that use white LEDs for backlighting, less than 10% of photons pass through polarizers, color filters, and other optical layers. Such optical losses can be partially avoided by using QD down-converters.

Solar concentrators are yet another technology that can use colloidal QDs as optical down-converters. QDs offer a promising way to reduce the cost of photovoltaic power by collecting solar radiation from a large area and “focusing” light onto a smaller, high-efficiency photovoltaic solar cell. The luminescent solar concentrators (LSCs) use QDs embedded in transparent thin-film waveguides to absorb the sunlight and reemit down-converted, red-shifted light, which is trapped in the high-refractive-index waveguide through total internal reflection. The concentrated, red-shifted light is guided to an edge of a LSC where the light is coupled to a high-efficiency solar cell. The efficiency of the simple one-layer device can be significantly enhanced by stacking multiple, transparent LSC layers using QDs emitting at different wavelengths.<sup>17</sup> Among

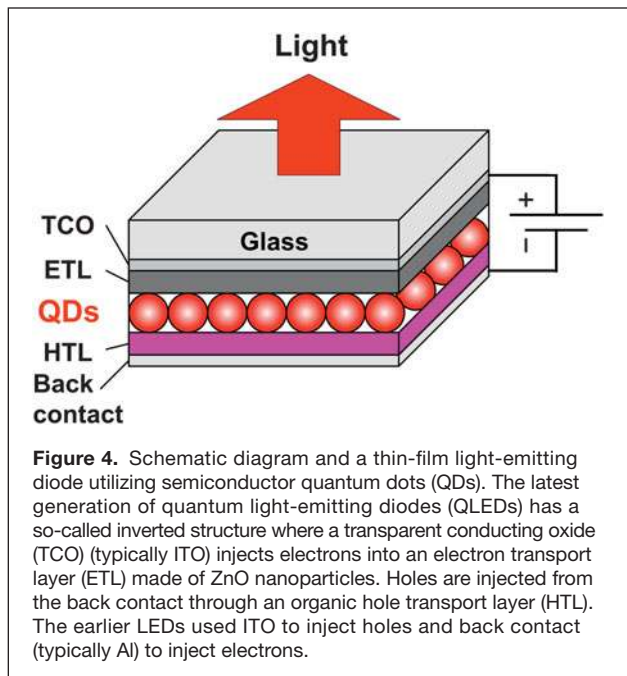
the advantages of LSCs are their low cost, light weight, flexibility, angle independence, and efficient operation under diffuse light conditions.

### Quantum dot light-emitting diodes

QLEDs, where electric current is used to directly excite QDs and generate electroluminescence, represent the next step in the utilization of QDs for light-emitting technologies.<sup>3,18–26</sup> The advantages of electrically driven QLEDs over the QD-based optical down-converters include: (1) the possibility of inexpensive, solution-based device fabrication and (2) the direct injection of carriers into QDs without energy losses during down-conversion, leading to potentially higher efficiency.

Colvin et al. reported on the first LEDs utilizing CdSe colloidal QDs in 1994.<sup>1</sup> External quantum efficiency ( $\eta_{ext}$ ), defined as the ratio of the number of photons emitted into free space to the number of injected charge carriers, of those first QLEDs was fairly low (0.001–0.01%) due to imbalanced carrier injection into the QDs and the low efficiency of the QDs themselves. Moreover, the EL spectra often combined light emission from the QDs and organic layers, negatively affecting the color purity. Since then, significant progress has been achieved in optimization of all components of the QLEDs.<sup>23,27,28</sup>

In a modern QLED, a layer of light-emitting QDs (e.g., CdSe/CdS core–shells or Cd<sub>1-x</sub>Zn<sub>x</sub>Se) is sandwiched between the hole transport layer (HTL) and electron transport layer (ETL), as shown in **Figure 4**. Using core–shell QDs as emitters allows for  $\eta_{ext}$  to significantly increase due to the enhanced efficiency of radiative recombination and greater tolerance of core–shell QDs to the processing conditions during device fabrication.<sup>18</sup> To achieve higher injection currents while avoiding the charging of QDs, optimally doped electron and HTLs were introduced, whereas the thickness of the emitting layer was reduced down to one or a few layers of highly luminescent QDs.<sup>27</sup>



When forward bias is applied to the device sketched in Figure 4, electrons and holes are injected into the nanocrystal layers from the ETL and HTL layers, respectively. The excitation of QDs occurs via two parallel processes: direct charge injection and exciton energy transfer from organic molecules. In direct charge injection, electrons may be trapped at the QDs as a result of the relative energy alignment of the lowest unoccupied molecular orbital (LUMO) levels of the HTL, ETL, and QDs (see the energy diagram in Figure 5a). For these charged QDs, the barrier to hole injection from the HTL is reduced. Upon acceptance of holes from HTL, excitons form on the QDs and subsequently recombine radiatively, delivering bright and color-saturated electroluminescence (Figure 5b–c). Alternately, excitons can be generated in organic molecules in close proximity to the QD layer. Non-radiative transfer of excitons from organic layers into the QDs solves the problem of imbalanced carrier injection and helps prevent QD charging.<sup>29</sup>

Optimization of ETL and HTL layers as well as the development of highly luminescent, stable, and, ideally, environmentally benign semiconductor QDs continue to be active areas of research. To date, most research has been carried out for

QLEDs with organic ETL and HTL layers that have been extensively studied by academic and industrial labs over the past decade.<sup>30</sup> Such devices have delivered  $\eta_{ext}$  of several percent with up to 10,000 cd/m<sup>2</sup> peak brightness. In 2012, impressive progress was achieved for devices with an inverted structure, where the ITO electrode injected electrons through an ETL made of ZnO nanoparticles, while holes were injected using an organic hole transport layer (Figure 5a).<sup>31,32</sup> These QLEDs, with an inverted structure and hybrid (inorganic/organic) injection layers, showed record  $\eta_{ext} \sim 18\%$ <sup>32</sup> and a peak brightness of >100,000 cd/m<sup>2</sup> (Reference 31) with lifetimes of hundreds of hours at 100 cd/m<sup>2</sup> brightness.

QLEDs can show bright and uniform emissions over large areas (e.g., see Figure 5c). Patterning of the QDs into pixels using transfer printing has also been demonstrated. In 2011, Samsung reported the first full-color QLED display with a 320 by 240 pixel array.<sup>33</sup>

### QLEDs: Future directions, markets, and prospects

After almost two decades of research and development, QLEDs are very close to full-scale commercialization (see the articles by Supran et al. and Kim et al. in this issue). Solution-based depositions of QDs and other layers bring down fabrication costs and allow for the use of flexible plastic substrates. Recent reports on brightness and efficiency of QLEDs demonstrated their competitiveness with other

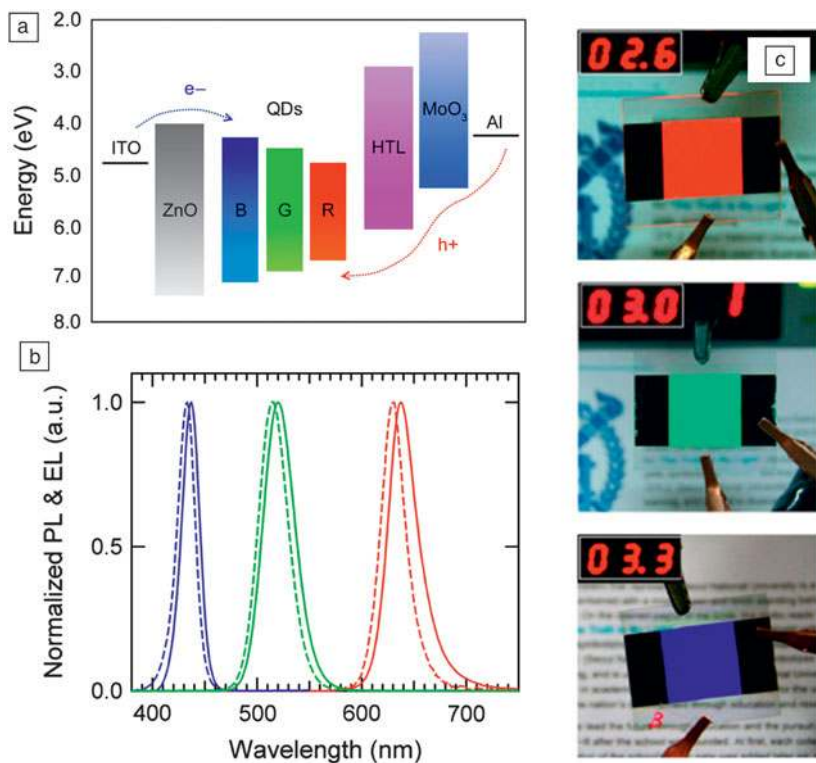


**Figure 5.** (a) Structure and energy level diagram of an inverted quantum light-emitting diode (QLED) where the layer of QDs emitted in blue (B), green (G), or red (R) is sandwiched between ZnO nanoparticles as the electron transport layer (ETL) and an organic hole transport layer (HTL). (b) Normalized photoluminescence spectra of QDs (dashed line) and electroluminescence spectra of QLEDs (solid line) with pure emission from QD layers. (c) Optical photographs of red, green, and blue LEDs. Bright, uniform, and defect-free emission from the QDs was observed over a large surface area (1.2 cm × 1.2 cm) at low applied voltage. Reprinted with permission from Reference 31. © 2011 American Chemical Society.

emerging display and solid-state lighting technologies. In terms of color purity, QLEDs easily outperform their immediate competitors, organic LEDs (OLEDs), but the commercial success of QLEDs will depend also on their ability to compete with OLEDs in stability, manufacturability, and other parameters. Further improvements of QLED efficiency and stability would require fundamental research toward better understanding of chemical and physical processes at the interfaces between QDs and organic or inorganic materials. This information will be necessary to optimize energy transfer and carrier injection from organic and inorganic layers into the QDs.

Thin-film QLEDs emitting white light can be used for large-area lighting systems and backlighting for liquid crystal displays. A number of labs reported white QLEDs with the emitting layer assembled of a balanced mixture of red, green, and blue emitting QDs.<sup>8</sup> Another promising niche market for QLEDs are the near-infrared (NIR)-emitting devices that are based on narrow gap semiconductors, such as InAs,<sup>34,35</sup> PbSe,<sup>36,37</sup> and HgTe.<sup>38</sup> Development of inexpensive, large-area NIR LEDs can address the needs of optical communications, chemical spectroscopy, and chemical sensing. Several research groups reported solution-processed QLEDs with emission bands at telecommunication wavelengths of 1.3  $\mu\text{m}$  and 1.55  $\mu\text{m}$ .<sup>34,39–41</sup> Various military applications can also provide a sizable market for NIR QLEDs.

### In this issue

This issue of *MRS Bulletin* covers a diverse range of topics related to the application of colloidal QDs for lighting technologies. These developments would be impossible without advancements of chemical synthesis of luminescent QDs, covered in the article by Chen et al. Scientists and engineers race to bring QDs into commercial solid-state lighting and consumer electronics. The articles by Supran et al. and Kim et al. discuss efforts along this way taken by the MIT, QD Vision, and Samsung teams, respectively. Supran et al. also look into the economic aspects of QD synthesis and discuss cost projections for manufacturing high-quality QDs. Optimizations of the efficiency and lifetime for QD devices requires a deep understanding of the recombination losses and degradation mechanisms. Bae et al. use state-of-the-art spectroscopy to look into carrier dynamics in QLEDs and suggest strategies for slowing non-radiative recombination in QLEDs at high driving currents. At the same time, Bozyigit and Wood discuss designs of novel QD structures and QLED architectures. Finally, Dang and Nurmikko look toward next-generation devices that use QDs as the lasing medium.

### Outlook

Impressive progress has been achieved in the development of robust and scalable procedures for synthesis of semiconductor quantum dots (QDs) with both high luminescence efficiency and narrow emissions. Future optimization of synthetic protocols toward perfect run-to-run reproducibility using less expensive and greener chemicals should bring the manufacturing costs

for high-quality QDs down toward \$10/g or less (see the article by Supran et al.). Since the use of less regulated materials may be necessary for some consumer products, special attention should be paid to the development of cadmium and lead-free QD materials. Serious attempts are being made to address this issue by developing luminescent QDs that do not contain toxic elements (e.g., InP/ZnS core–shells<sup>42,43</sup> or CuInSe<sub>2</sub><sup>44,45</sup>). Very recently, Si QDs have been used in LED devices, showing that strong quantum confinement allows for the use of silicon in a very unexpected capacity of a light emitter.<sup>46,47</sup>

High-performance devices will require the optimization of many competing parameters. System engineering will require a more substantial effort in order to gain a complete understanding of charge injection and degradation mechanisms in QLEDs under operational conditions. It has been recently shown that thermal conductivity of QD layers can be orders of magnitude lower than that of traditional semiconductors.<sup>48</sup> The optimization of thermal management in QLEDs offers a promising direction toward improved stability, efficiency, and brightness. One should also look beyond using organic molecules as surface ligands for QDs—inorganic and hybrid ligands for colloidal NCs could provide an interparticle medium that is more thermally conductive and/or transparent for charge carriers. Optimization of all-inorganic QLEDs can bring QD devices closer in performance to single-crystal LEDs while maintaining low manufacturing costs. Strong electronic coupling between neighboring QDs can lead to the formation of collective electronic states (minibands).<sup>49</sup> Such materials have not yet been explored for LED applications, but they may provide an interesting opportunity, especially for device operation at high injection currents (e.g., in future electrically pumped QD lasers).

### Acknowledgments

The guest editors are grateful to Seth Coe-Sullivan, Charlie Hamilton, and John Ho for advice and stimulating discussions. D.V.T. thanks the University of Chicago NSF MRSEC Program under Award Number DMR-0213745, the Keck Foundation, and the David and Lucile Packard Fellowship for support of research on quantum dots.

### References

1. L. Brus, *J. Phys. Chem.* **90**, 2555 (1986).
2. A.L. Efros, A.L. Efros, *Sov. Phys. Semicond.* **16**, 772 (1982).
3. V.L. Colvin, M.C. Schlamp, A.P. Alivisatos, *Nature* **370**, 354 (1994).
4. J.M. Bruchez, M. Moronne, P. Gin, S. Weiss, A.P. Alivisatos, *Science* **281**, 2013 (1998).
5. D.V. Talapin, I. Mekis, S. Götzinger, A. Kornowski, O. Benson, H. Weller, *J. Phys. Chem. B* **108**, 18826 (2004).
6. P. Reiss, J. Bleuse, A. Pron, *Nano Lett.* **2**, 781 (2002).
7. L. Qu, X. Peng, *J. Am. Chem. Soc.* **124**, 2049 (2002).
8. P.O. Anikeeva, J.E. Halpert, A.G. Bawendi, V. Bulović, *Nano Lett.* **7**, 2196 (2007).
9. X. Peng, M.C. Schlamp, A.V. Kadavanich, A.P. Alivisatos, *J. Am. Chem. Soc.* **119**, 7019 (1997).
10. D.V. Talapin, A.L. Rogach, M. Haase, H. Weller, *J. Phys. Chem. B* **105**, 12278 (2001).
11. C.B. Murray, D.J. Norris, M.G. Bawendi, *J. Am. Chem. Soc.* **115**, 8706 (1993).
12. O. Chen, J. Zhao, V.P. Chauhan, J. Cui, C. Wong, D.K. Harris, H. Wei, H.-S. Han, D. Fukumura, R.K. Jain, M.G. Bawendi, *Nat. Mater.* **12**, 445 (2013).

13. R. Xie, U. Kolb, J. Li, T. Basché, A. Mews, *J. Am. Chem. Soc.* **127**, 7480 (2005).
14. M. Achermann, M.A. Petruska, S. Kos, D.L. Smith, D.D. Koleske, V.I. Klimov, *Nature* **429**, 642 (2004).
15. J. Lee, V.C. Sundar, J.R. Heine, M.G. Bawendi, K.F. Jensen, *Adv. Mater.* **12**, 1102 (2000).
16. S. Nizamoglu, T. Ozel, E. Sari, H.V. Demir, *Nanotechnology*. **18**, 065709 (2007).
17. A.J. Chatten, K.W.J. Barnham, B.F. Buxton, N.J. Ekins-Daukes, M.A. Malik, *Semicond.* **38**, 909 (2004).
18. M.C. Schlamp, X.G. Peng, A.P. Alivisatos, *J. Appl. Phys.* **82**, 5837 (1997).
19. H. Mattoussi, L.H. Radzilowski, B.O. Dabbousi, E.L. Thomas, M.G. Bawendi, M.F. Rubner, *J. Appl. Phys.* **83**, 7965 (1998).
20. S. Chaudhary, M. Ozkan, W.C.W. Chan, *Appl. Phys. Lett.* **84**, 2925 (2004).
21. S. Coe-Sullivan, J.S. Steckel, W.K. Woo, M.G. Bawendi, V. Bulovic, *Adv. Funct. Mater.* **15**, 1117 (2005).
22. J.S. Steckel, P. Snee, S. Coe-Sullivan, J.P. Zimmer, J.E. Halpert, P. Anikeeva, L.A. Kim, V. Bulovic, M.G. Bawendi, *Angew. Chem. Int. Ed.* **45**, 5796 (2006).
23. J.M. Caruge, J.E. Halpert, V. Bulović, M.G. Bawendi, *Nano Lett.* **6**, 2991 (2006).
24. Q. Sun, Y.A. Wang, L.S. Li, D. Wang, T. Zhu, J. Xu, C. Yang, Y. Li, *Nat. Photon.* **1**, 717 (2007).
25. A.H. Mueller, M.A. Petruska, M. Achermann, D.J. Werder, E.A. Akhadov, D.D. Koleske, M.A. Hoffbauer, V.I. Klimov, *Nano Lett.* **5**, 1039 (2005).
26. S. Coe-Sullivan, W.-K. Woo, J.S. Steckel, M. Bawendi, V. Bulović, *Org. Electron.* **4**, 123 (2003).
27. S. Coe, W.-K. Woo, M. Bawendi, V. Bulovic, *Nature* **420**, 800 (2002).
28. J. Zhao, J.A. Bardecker, A.M. Munro, M.S. Liu, Y. Niu, I.K. Ding, J. Luo, B. Chen, A.K.Y. Jen, D.S. Ginger, *Nano Lett.* **6**, 463 (2006).
29. P.O. Anikeeva, C.F. Madigan, J.E. Halpert, M.G. Bawendi, V. Bulović, *Phys. Rev. B* **78**, 085434 (2008).
30. Y. Shirasaki, G.J. Supran, M.G. Bawendi, V. Bulović, *Nat. Photonics* **7**, 13 (2013).
31. J. Kwak, W.K. Bae, D. Lee, I. Park, J. Lim, M. Park, H. Cho, H. Woo, D.Y. Yoon, K. Char, S. Lee, C. Lee, *Nano Lett.* **12**, 2362 (2012).
32. B.S. Mashford, M. Stevenson, Z. Popovic, C. Hamilton, Z. Zhou, C. Breen, J. Steckel, V. Bulović, M. Bawendi, S. Coe-Sullivan, P.T. Kazlas, *Nature Photon* **7**, 407 (2013).
33. T.-H. Kim, K.-S. Cho, E.K. Lee, S.J. Lee, J. Chae, J.W. Kim, D.H. Kim, J.-Y. Kwon, G. Amaratunga, S.Y. Lee, B.L. Choi, Y. Kuk, J.M. Kim, K. Kim, *Nat. Photonics* **5**, 176 (2011).
34. A.L. Rogach, A. Eychmuller, S.G. Hickey, S.V. Kershaw, *Small* **3**, 536 (2007).
35. R.D. Schaller, J.M. Pietryga, V.I. Klimov, *Nano Lett.* **7**, 3469 (2007).
36. A. Sashchiuk, L. Amirav, M. Bashouti, M. Krueger, U. Sivan, E. Lifshitz, *Nano Lett.* **4**, 159 (2004).
37. K.S. Cho, D.V. Talapin, W. Gaschler, C.B. Murray, *J. Am. Chem. Soc.* **127**, 7140 (2005).
38. A.L. Rogach, D.S. Koktysh, M. Harrison, N.A. Kotov, *Chem. Mater.* **12**, 1526 (2000).
39. N. Tessler, V. Medvedev, M. Kazes, S. Kan, U. Banin, *Science* **295**, 1506 (2002).
40. Y.Q. Li, A. Rizzo, R. Cingolani, G. Gigli, *Microchim. Acta* **159**, 207 (2007).
41. A.L. Rogach, N. Gaponik, J.M. Lupton, C. Bertoni, D.E. Gallardo, S. Dunn, N.L. Pira, M. Paderi, P. Repetto, S.G. Romanov, C. O'Dwyer, C.M. Sotomayor Torres, A. Eychmüller, *Angew. Chem. Int. Ed.* **47**, 6538 (2008).
42. L. Li, P. Reiss, *J. Am. Chem. Soc.* **130**, 11588 (2008).
43. J. Ziegler, S. Xu, E. Kucur, F. Meister, M. Batentschuk, F. Gindele, T. Nann, *Adv. Mater.* **20**, 4068 (2008).
44. R.P. Raffaele, S.L. Castro, A.F. Hepp, S.G. Bailey, *Prog. Photovolt.* **10**, 433 (2002).
45. M.A. Malik, P. O'Brien, N. Revaprasadu, *Adv. Mater.* **11**, 1441 (1999).
46. K.-Y. Cheng, R. Anthony, U.R. Kortshagen, R.J. Holmes, *Nano Lett.* **11**, 1952 (2011).
47. F. Maier-Flaig, J. Rinck, M. Stephan, T. Bocksrocker, M. Bruns, C. Kübel, A.K. Powell, G.A. Ozin, U. Lemmer, *Nano Lett.* **13**, 475 (2013).
48. W.L. Ong, S.M. Rupich, D.V. Talapin, A.J.H. McGaughey, J.A. Malen, *Nat. Mater.* **12**, 410 (2013).
49. O.L. Lazarenkova, A.A. Balandin, *J. Appl. Phys.* **89**, 5509 (2001).
50. A.L. Rogach, D.V. Talapin, E.V. Shevchenko, A. Kornowski, M. Haase, H. Weller, *Adv. Funct. Mater.* **12**, 653 (2002).
51. E.F. Schubert, *Light-Emitting Diodes* (Cambridge University Press, Cambridge, UK, 2006).
52. <http://dot-color.com/tag/cie-1931/>.
53. <http://www.qdvision.com/content1566>. □

## High Resolution RBS

National Electrostatics Corporation has added Ångstrom level, High Resolution RBS to the RC43 Analysis System for nanotechnology applications. A single Pelletron instrument can now provide RBS, channeling RBS, microRBS, PIXE, ERDA, NRA, and HR-RBS capability, collecting up to four spectra simultaneously. Pelletron accelerators are available with ion beam energies from below 1 MeV in to the 100 MeV region.

[www.pelletron.com](http://www.pelletron.com)

Phone: 608-831-7600

E-mail: [nec@pelletron.com](mailto:nec@pelletron.com)

Full wafer version of the model RC43 analysis end station with High Resolution RBS Detector.

**National Electrostatics Corp.**